

1 **Variation in supplemental carbon dioxide requirements defines lineage-specific antibiotic
2 resistance acquisition in *Neisseria gonorrhoeae***

3
4 Daniel H.F. Rubin¹, Kevin C. Ma¹, Kathleen A. Westervelt¹, Karthik Hullahalli^{2,3}, Matthew K. Wal-
5 dor^{1,2,3}, Yonatan H. Grad^{1,2}

6
7 Affiliations
8 [1] Department of Immunology and Infectious Diseases, Harvard T.H. Chan School of Public
9 Health, Boston, MA, USA

10 [2] Division of Infectious Diseases, Brigham and Women's Hospital, Harvard Medical School,
11 Boston, MA, USA

12 [3] Department of Microbiology, Harvard Medical School, Boston, MA, USA

13
14

15 Corresponding author
16 Yonatan Grad
17 Department of Immunology and Infectious Diseases
18 Harvard T.H. Chan School of Public Health
19 665 Huntington Ave.

20 Building 1, Room 715
21 Boston, MA, 02115
22

23 Contact information
24 Email: ygrad@hsph.harvard.edu; tel: 617-432-2275
25

26 **Abstract**

27 The evolution of the obligate human pathogen *Neisseria gonorrhoeae* has been shaped
28 by selective pressures from diverse host niche environments^{1,2} as well as antibiotics^{3,4}. The var-
29 ying prevalence of antibiotic resistance across *N. gonorrhoeae* lineages⁵ suggests that underlying
30 metabolic differences may influence the likelihood of acquisition of specific resistance muta-
31 tions^{6,7}. We hypothesized that the requirement for supplemental CO₂, present in approximately
32 half of isolates⁸, reflects one such example of metabolic variation. Here, using a genome-wide
33 association study and experimental investigations, we show that CO₂-dependence is attributable
34 to a single substitution in a β-carbonic anhydrase, *canB*. CanB^{19E} is necessary and sufficient for
35 growth in the absence of CO₂, and the hypomorphic CanB^{19G} variant confers CO₂-dependence.
36 Furthermore, ciprofloxacin resistance is correlated with CanB^{19G} in clinical isolates, and the pres-
37 ence of CanB^{19G} increases the likelihood of acquisition of ciprofloxacin resistance. Together, our
38 results suggest that metabolic variation has impacted the acquisition of fluoroquinolone re-
39 sistance.

40 **Main Text**

41 *N. gonorrhoeae* is commonly cultured in the presence of supplemental CO₂⁹, though the
42 molecular basis for this trait has not been elucidated. We first investigated the mechanism of CO₂-
43 dependence using a genome-wide association study (GWAS). To generate phenotypes for
44 GWAS, clinical and laboratory strains of *N. gonorrhoeae* were assessed for growth in the pres-
45 ence and absence of supplemental CO₂. The GWAS revealed a significant association with a
46 single genomic site, a missense mutation in *ngo2079* (**Fig. 1A**). In a parallel unbiased method,
47 genomic DNA from FA6140, an *N. gonorrhoeae* strain that does not depend on supplemental
48 CO₂, was used to transform FA19, a lab isolate that requires supplemental CO₂ (**Supp. Fig. 1A**).
49 Transformants that grew in the absence of supplemental CO₂ had acquired multiple SNPs in the
50 region of *ngo2079* (**Supp. Fig. 1B, C**), including the SNP identified by GWAS.

51 The *ngo2079* c.56G→A SNP encodes a G→E mutation at amino acid 19 of NGO2079, a
52 β-carbonic anhydrase. *N. gonorrhoeae* contains two additional carbonic anhydrases: a well-char-
53 acterized essential periplasmic α-carbonic anhydrase¹⁰⁻¹² and a putative nonessential cytosolic γ-
54 carbonic anhydrase¹³. All carbonic anhydrases catalyze the conversion of H₂O and gaseous CO₂
55 to aqueous bicarbonate. Aqueous bicarbonate is then used as a carbon building block in multiple
56 pathways within the cell, including the synthesis of TCA cycle components, nucleotides, and phos-
57 pholipids¹⁴ (**Supp. Fig. 1C**). As *ngo2079* is the sole predicted *N. gonorrhoeae* β-carbonic anhy-
58 drase, we named this gene *canB* to parallel the corresponding carbonic anhydrase *can* in *E. coli*.
59 The SNP is located outside of the highly conserved carbonic anhydrase domain (**Supp. Fig. 1D**)
60 and does not appear to be within a signal sequence domain by SignalP¹⁵. Structures from Al-
61 phafold¹⁶ indicate that the variant amino acid lies between two N-terminal alpha-helices, but it
62 does not appear at the dimerization interface or the characterized active site (**Supp. Fig. 1E**).

63 We validated our GWAS results by introducing the CanB variants into *N. gonorrhoeae*.
64 Replacement by kanamycin co-selection of the CanB^{19E} in FA1090 with CanB^{19G} and of the
65 CanB^{19G} in FA19 with CanB^{19E} showed that dependence on supplemental CO₂ was attributable
66 to CanB^{19G} (**Fig. 1B**), while similar results for single point mutants in 28BL (19E→G) and FA19
67 (19G→E) (**Fig. 1C**) support this idea. These results indicate that CanB^{19E} is both necessary and
68 sufficient for growth in the absence of supplemental CO₂. The concentration of CO₂ that differen-
69 tiates this dependency is between atmospheric (~410 ppm) and 0.1% CO₂ (1000 ppm) (**Supp.**
70 **Fig. 2A**), slightly lower than has been found in other bacteria¹⁷ and considerably below the 5%
71 CO₂ standardly used in *N. gonorrhoeae* growth protocols⁹.

72 CanB^{19G}, the allele that confers CO₂-dependence, appears to have arisen multiple times
73 in *N. gonorrhoeae*, whereas genomes from *Neisseria* spp. and other closely related bacteria en-
74 code only CanB^{19E} (**Fig. 1D**). Analysis of the PubMLST database of more than 36,000 *Neisseria*
75 spp. genomes showed that only one non-gonococcal *Neisseria* isolate carries CanB^{19G}, a urethral
76 isolate of *N. meningitidis* (PubMLST id: 82427) that appears to have acquired the *canB* region

77 from *N. gonorrhoeae* (100% identity to sequenced *N. gonorrhoeae* isolates). Within *N. gonor-*
78 *rhoeae*, ~50% of sequenced isolates from across the phylogenetic tree have CanB^{19G} (**Fig. 1D,**
79 **E**). The proportion of sequenced isolates with CanB^{19G} has remained relatively stable at ~50%
80 during last twenty years (**Supp. Fig. 6A**), though this allele appears to have been less common
81 in the pre-antibiotic era of the 1930s (9% of pre-1930 *N. gonorrhoeae* isolates from the PubMLST
82 database).

83 Although CanB^{19E} provides a growth advantage in the absence of supplemental CO₂, the
84 growth of FA19 CanB^{19G} and CanB^{G19E} in the presence of supplemental CO₂ was indistinguishable
85 and independent of inoculum size (**Fig. 1F, left**). Furthermore, in the presence of CO₂, kanamycin-
86 labeled CanB isogenic FA19 strains remained at equal proportions in competition (**Supp. Fig.**
87 **2B**). The CanB^{19G} variant, therefore, does not confer a general fitness defect but a specific growth
88 disadvantage in the absence of CO₂. As shown in **Fig. 1F, right**, this disadvantage is concentra-
89 tion-dependent and is exacerbated at lower starting inocula. Although FA19 CanB^{19E} is able to
90 grow at all starting CO₂ concentrations, both strains have a substantially longer lag phase in the
91 absence of CO₂, suggesting that intracellular bicarbonate plays a critical role in lag phase, similar
92 to *N. meningitidis*¹⁸. This competitive disadvantage is not rescued by extracellular sodium bicar-
93 bonate or oxaloacetate, a downstream product of intracellular bicarbonate (**Supp. Fig. 2C**). Thus,
94 in contrast to many bacteria that are able to acquire bicarbonate from the environment via inor-
95 ganic carbon transporters¹⁹, *N. gonorrhoeae* does not appear to have a CO₂-concentrating mech-
96 anism apart from cytosolic carbonic anhydrases, explaining why exogenous bicarbonate does not
97 rescue the competition defect. Supplementation with metabolites downstream of intracellular bi-
98 carbonate (**Supp. Fig. 1D**), such as pyruvate, sub-minimum inhibitory concentration (MIC) pal-
99 mitic acid, and purines were also unable to rescue this defect (**Supp. Fig. 2D**).

100 *E. coli* MG1655 was used to compare the activity of the CanB variants. Deletion of one of
101 the two endogenous *E. coli* β -carbonic anhydrases, *can*, rendered MG1655 capnophilic and de-
102 pendent on supplemental CO₂ (**Fig. 2A**, top two quadrants). Complementation with IPTG-

103 inducible *N. gonorrhoeae* CanB variants restored growth in the absence of supplemental CO₂.
104 However, lower concentrations of IPTG were required for complementation with CanB^{19E} versus
105 CanB^{19G} (**Fig. 2B**, lower two quadrants), even though the abundance of CanB^{19E} and CanB^{19G}
106 were similar at equivalent levels of induction (**Supp. Fig. 3A**), suggesting that CanB^{19G} retains
107 some enzymatic activity but does not restore growth as efficiently as CanB^{19E}.

108 Since CanB^{19G} is a hypomorph, we hypothesized that the CanB variants result in altered
109 gonococcal physiology. At pH 4.5, an acidic condition similar to healthy vaginal pH²⁰, FA19
110 CanB^{19G} died more quickly than the isogenic FA19 CanB^{19E} (**Fig. 2B, C**), consistent with the find-
111 ing that, in the absence of supplemental CO₂, FA19 CanB^{19G} is less able to buffer intracellular pH
112 (**Fig. 2D**). The CanB^{19E} survival advantage at low pH did not extend, however, to intracellular
113 survival within immortalized macrophages (**Supp. Fig. 4A**). At higher pH and in aerobic condi-
114 tions, neither the CanB^{19E} or CanB^{19G} variant displayed a substantial advantage (**Supp. Fig. 2B**,
115 **Supp. Fig. 4B**). In contrast, in anaerobic conditions, FA19 CanB^{19E} had a distinct growth ad-
116 vantage across the pH range supportive of growth (**Fig. 2E**, **Supp. Fig. 4C**). Our data thus show
117 that the CanB^{19E} allele provides an advantage at low pH and under anaerobic conditions, sug-
118 gesting that CanB^{19E} may allow for buffering in the acidic vaginal environment.

119 Carbonic anhydrases have been previously shown to be targets of sulfa antibiotics¹² and
120 to mediate natural competence in *N. meningitidis*²¹. Sulfa antibiotics were one of the first antibiot-
121 ics to be used to treat gonorrhea²² and primarily target dihydropteroate synthase in the folate
122 synthesis pathway. Both CanB variants had similar sulfamethoxazole and trimethoprim/sulfa-
123 methoxazole MICs across two genetic backgrounds (**Supp. Table 2A**). Furthermore,
124 MG1655Δcan complemented with CanB^{19G} or CanB^{19E} also had similar sulfamethoxazole MICs
125 (**Supp. Table 2B**). The CanB variants therefore do not have different susceptibility to sulfa anti-
126 biotics. With respect to competence, a *canB* knockout was dependent on supplemental CO₂
127 (**Supp. Fig. 5A**), but both the wild-type and knockout had the same level of natural competence,
128 as measured by the introduction of a single SNP in *gyrB* conferring nalidixic acid resistance

129 (**Supp. Fig. 5B**). Similarly, competence was not associated with the CanB isogenic pairs of FA19
130 and 28BL (**Supp. Fig. 5B**). Thus, selection for CanB variants does not appear to be driven by
131 associations with sulfa susceptibility or natural competence.

132 In *N. gonorrhoeae*, antibiotic resistance varies across the phylogenetic tree, with some
133 lineages displaying more resistance than others, though the reasons explaining these differences
134 are not known. One hypothesis is that lineages may be subject to demographically or geograph-
135 ically variable antibiotic pressures. The overrepresentation of heterosexuals in Lineage B and
136 men-who-have-sex-with-men in Lineage A lend support to this hypothesis⁵ (**Figure 1E**), but the
137 rapid global spread of *N. gonorrhoeae* and the extensive bridging across sexual networks argue
138 against it²³. Alternatively, we hypothesized that genomic and associated metabolic variation could
139 modify the likelihoods of acquiring and maintaining resistance. Support for this idea comes from
140 previous research showing that intracellular metabolite perturbations can shape the likelihood of
141 developing resistance^{24,25}. To begin to address whether the CanB variants have shifted the evo-
142 lutionary landscape of *N. gonorrhoeae* antibiotic resistance, we analyzed whether the variants are
143 associated with antibiotic resistance on the population level. We found that the CanB^{19G} variant is
144 associated with >4-fold higher MICs for ciprofloxacin (average log₂ MIC 0.43 vs. 0.10 µg/mL) (**Fig.**
145 **3A**), whereas MICs for azithromycin (0.32 µg/mL vs. 0.24 µg/mL), penicillin (0.41 vs. 0.70 µg/mL),
146 and ceftriaxone (.0093 µg/mL vs. .013 µg/mL) did not differ (**Supp. Fig. 6B**). CanB^{19G} is also
147 associated with the most common resistance determinant for ciprofloxacin, GyrA^{91F}, as 52.3% of
148 CanB^{19G} isolates have GyrA^{91F}, as compared to only 30.4% of CanB^{19E} isolates (p<0.0001, Pear-
149 son's chi-square) (**Fig. 3B**). This relationship holds true across years, as the proportion of GyrA^{91F}
150 and CanB^{19G} isolates per year in the United States have tracked closely since 2000 (**Fig. 3C**). On
151 a country-by-country level, isolates with CanB^{19G} have a comparatively higher ciprofloxacin MIC
152 (**Supp. Fig. 6C**), indicating that the association is true across datasets and geography. The sim-
153 plest explanation is that CanB^{19G} directly increases ciprofloxacin resistance. However, the iso-
154 genic CanB FA19 strains have comparable levels of resistance to ciprofloxacin (**Supp. Table 2C**).

155 We therefore theorized that the CanB^{19G} allele may lead to a greater rate of acquisition of
156 ciprofloxacin-specific resistance. A fluctuation assay to estimate the mutation rate to different an-
157 tibiotics was used to test this idea. FA19 CanB^{19G} had a significantly higher mutation rate than
158 FA19 CanB^{19E} when plated on ciprofloxacin (**Fig. 3D**). Furthermore, the fold-change in mutation
159 rate remained similar following preincubation with sub-MIC ciprofloxacin, which is known to in-
160 crease the rate of mutation and acquisition of resistance²⁶. This suggests that it is not exposure
161 to ciprofloxacin itself that mediates the difference between CanB^{19G} and CanB^{19E}, but rather a
162 difference in the pre-exposure populations. There was no difference in killing by ciprofloxacin for
163 either strain, providing further evidence that the difference in mutation rate is not due to differential
164 viability in the presence of drug (**Supp. Fig. 7A**).

165 We reasoned that there were two potential explanations for the differences in ciprofloxacin
166 mutation rates associated with the CanB^{19G} and CanB^{19E} variant strains. The first is that there is
167 a difference in basal mutation rate between the strains, manifesting as a higher rate of resistance
168 to all antibiotics. This does not appear to be the case, since isogenic CanB FA19 strains had very
169 similar mutation rates to rifampin, an antibiotic that targets RNA polymerase (**Fig. 3D**). Further-
170 more, a similar fluctuation assay in *E. coli* showed that induction of CanB^{19G} led to a higher rate
171 of ciprofloxacin-specific resistance acquisition (**Supp. Fig. 3B**).

172 A second possibility is that the CanB^{19G} strains have an increased ability to tolerate *gyrA*
173 mutations. If this were true, we would expect that CanB^{19E} *gyrA* mutants would have a relative
174 competitive disadvantage compared to the parental strains. To investigate this possibility, we
175 generated GyrA^{91F} and GyrA^{91F/95G} mutants in both FA19 CanB backgrounds. For both the GyrA^{91F}
176 and GyrA^{91F/95G} mutants, the CanB^{19E} strain was significantly disadvantaged against the parental
177 strain (**Fig. 3E**). In monoculture, FA19 CanB^{19E} GyrA^{91F/95G} also grew significantly slower than
178 FA19 CanB^{19G} GyrA^{91F/95G} (**Fig. 3F**), as did the equivalent mutants in the 28BL background (**Supp.**
179 **Fig. 7B**). We generated spontaneous ciprofloxacin resistant mutants, all of which bore GyrA⁹⁵
180 variants seen in clinical isolates (**Supp. Table 2D**). The ciprofloxacin-resistant FA19 CanB^{19G}

181 strains competed better than ciprofloxacin-resistant CanB^{19E} strains against the susceptible pa-
182 rental strains (**Supp. Fig. 7C**) and showed faster growth in monoculture (**Supp. Fig. 7D**). Taken
183 together, these results suggest that the increased rate of acquisition of ciprofloxacin resistance in
184 the CanB^{19G} background is due to its higher relative fitness in the background of gyrase mutations.

185 Collectively, our findings suggest that CanB represents a novel metabolic mediator of drug
186 resistance acquisition. Although canB is not essential for *in vitro* growth (**Supp. Fig. 5A**), we ob-
187 served no evidence of premature stop codons in a collection of >16,000 genomes from clinical
188 isolates, indicating its important role *in vivo*. The hypomorphic CanB^{19G} allele is present almost
189 exclusively in *N. gonorrhoeae* among the *Neisseriae* and can be found in samples predating the
190 introduction of antibiotics, suggesting it reflects adaptation to the urogenital niche or sexual trans-
191 mission. CanB^{19E} also shows lineage-specific background dependence, as the alleviation of CO_2 -
192 dependence in clinical isolate NY0195 requires further introduction of AasN^{Q321E} , a mutation in an
193 acyl-ACP synthetase involved in fatty acid uptake²⁷ (**Supp. Fig. 8A**). The AasN^{321Q} variant is re-
194 stricted to a single lineage that carries the ceftriaxone-resistance determining PenA34 allele
195 (**Supp. Fig. 8B**), suggesting further complex connections between central metabolism and anti-
196 biotic resistance.

197 CanB^{19G} is therefore an example of a widespread variant that facilitates acquisition of drug-
198 specific resistance through shifts in the gonococcal metabolic landscape and without directly af-
199 fecting drug susceptibility or tolerance. This finding expands upon recent work showing that mu-
200 tations in important metabolic genes can change the drug-specific resistance profile of clinical
201 isolates.⁶ By showing how specific lineages are more likely to acquire specific resistance deter-
202 minants, our work provides a new perspective for understanding the evolution of antibiotic re-
203 sistance.

204

205 **Author contributions**

206 DHFR and KCM performed the GWAS and statistical analyses. DHFR and KAW performed the
207 anaerobic experiments. DHFR and KH performed the macrophage experiments. The remainder
208 of the experimental work was performed by DHFR. All authors (DHFR, KCM, KAW, KH, MKW,
209 YHG) contributed to data interpretation. YHG supervised and managed the study. DHFR and
210 YHG wrote the manuscript. All authors reviewed and edited the final manuscript. All authors were
211 responsible for the decision to submit for publication.

212 **Acknowledgements**

213 We thank the members of the Grad Lab and the Waldor lab for their invaluable feedback into this
214 project; Samantha Palace in particular for her thoughts on experimental design; and the Microbial
215 Genome Sequencing Center (<https://www.migscenter.com/>) for their work sequencing strains.
216 This work was supported by NIH R01 AI132606 and R01 AI153521 and by the Smith Family
217 Foundation Odyssey award (YHG) and R01 AI 042347-24 (MKW). DHFR is funded by NIH F30
218 AI160911-01 and NIH T32 GM007753. KH is supported by NIH F31 AI156949-01.

219 **Competing interests**

220 YHG is on the Scientific advisory board of Day Zero Diagnostics and consults for GSK. YHG
221 has received funding from Merck and Pfizer. None of these competing interests has a bearing
222 on this project.

References

223
224
225 1 Ma, K. C. *et al.* Adaptation to the cervical environment is associated with increased
226 antibiotic susceptibility in *Neisseria gonorrhoeae*. *Nat Commun* **11**, 4126,
227 doi:10.1038/s41467-020-17980-1 (2020).
228 2 Lewis, L. A. & Ram, S. Complement interactions with the pathogenic Neisseriae:
229 clinical features, deficiency states, and evasion mechanisms. *FEBS Lett* **594**,
230 2670-2694, doi:10.1002/1873-3468.13760 (2020).
231 3 Palace, S. G. *et al.* RNA polymerase mutations cause cephalosporin resistance in
232 clinical *Neisseria gonorrhoeae* isolates. *eLife* **9**, doi:10.7554/eLife.51407 (2020).
233 4 Golparian, D. *et al.* Genomic evolution of *Neisseria gonorrhoeae* since the
234 preantibiotic era (1928-2013): antimicrobial use/misuse selects for resistance and
235 drives evolution. *BMC genomics* **21**, 116, doi:10.1186/s12864-020-6511-6 (2020).
236 5 Sánchez-Busó, L. *et al.* The impact of antimicrobials on gonococcal evolution.
237 *Nature Microbiology* **4**, 1941-1950, doi:10.1038/s41564-019-0501-y (2019).
238 6 Lopatkin, A. J. *et al.* Clinically relevant mutations in core metabolic genes confer
239 antibiotic resistance. *Science (New York, N.Y.)* **371**, doi:10.1126/science.aba0862
240 (2021).
241 7 Ford, C. B. *et al.* *Mycobacterium tuberculosis* mutation rate estimates from
242 different lineages predict substantial differences in the emergence of drug-
243 resistant tuberculosis. *Nat Genet* **45**, 784-790, doi:10.1038/ng.2656 (2013).
244 8 Platt, D. J. Carbon dioxide requirement of *Neisseria gonorrhoeae* growing on a
245 solid medium. *J Clin Microbiol* **4**, 129-132 (1976).
246 9 Dillard, J. P. Genetic Manipulation of *Neisseria gonorrhoeae*. *Current protocols in*
247 *microbiology* **0 4**, Unit4A.2, doi:10.1002/9780471729259.mc04a02s23 (2011).
248 10 Huang, S. *et al.* Crystal structure of carbonic anhydrase from *Neisseria*
249 *gonorrhoeae* and its complex with the inhibitor acetazolamide. *J Mol Biol* **283**, 301-
250 310, doi:10.1006/jmbi.1998.2077 (1998).
251 11 Elleby, B., Chirica, L. C., Tu, C., Zeppezauer, M. & Lindskog, S. Characterization
252 of carbonic anhydrase from *Neisseria gonorrhoeae*. *Eur J Biochem* **268**, 1613-
253 1619 (2001).
254 12 Hewitt, C. S. *et al.* Structure-Activity Relationship Studies of Acetazolamide-Based
255 Carbonic Anhydrase Inhibitors with Activity against *Neisseria gonorrhoeae*. *ACS*
256 *Infect Dis* **7**, 1969-1984, doi:10.1021/acsinfecdis.1c00055 (2021).
257 13 Remmeli, C. W. *et al.* Transcriptional landscape and essential genes of *Neisseria*
258 *gonorrhoeae*. *Nucleic Acids Res* **42**, 10579-10595, doi:10.1093/nar/gku762
259 (2014).
260 14 Merlin, C., Masters, M., McAteer, S. & Coulson, A. Why is carbonic anhydrase
261 essential to *Escherichia coli*? *Journal of bacteriology* **185**, 6415-6424,
262 doi:10.1128/jb.185.21.6415-6424.2003 (2003).
263 15 Teufel, F. *et al.* SignalP 6.0 predicts all five types of signal peptides using protein
264 language models. *Nature biotechnology*, doi:10.1038/s41587-021-01156-3
265 (2022).
266 16 Jumper, J. *et al.* Highly accurate protein structure prediction with AlphaFold.
267 *Nature* **596**, 583-589, doi:10.1038/s41586-021-03819-2 (2021).

268 17 Burghout, P. *et al.* A single amino acid substitution in the MurF UDP-MurNAc-
269 pentapeptide synthetase renders *Streptococcus pneumoniae* dependent on CO₂
270 and temperature. *Molecular microbiology* **89**, 494-506, doi:10.1111/mmi.12292
271 (2013).

272 18 Tuttle, D. M. & Scherp, H. W. Studies on the carbon dioxide requirement of
273 *Neisseria meningitidis*. *Journal of bacteriology* **64**, 171-182,
274 doi:10.1128/jb.64.2.171-182.1952 (1952).

275 19 Fan, S. H. *et al.* MpsAB is important for *Staphylococcus aureus* virulence and
276 growth at atmospheric CO(2) levels. *Nature communications* **10**, 3627,
277 doi:10.1038/s41467-019-11547-5 (2019).

278 20 Linhares, I. M., Summers, P. R., Larsen, B., Giraldo, P. C. & Witkin, S. S.
279 Contemporary perspectives on vaginal pH and lactobacilli. *American journal of
280 obstetrics and gynecology* **204**, 120.e121-125, doi:10.1016/j.ajog.2010.07.010
281 (2011).

282 21 Muir, A. *et al.* Construction of a complete set of *Neisseria meningitidis* mutants and
283 its use for the phenotypic profiling of this human pathogen. *Nature communications*
284 **11**, 5541, doi:10.1038/s41467-020-19347-y (2020).

285 22 Kampmeier, R. H. Introduction of sulfonamide therapy for gonorrhea. *Sexually
286 transmitted diseases* **10**, 81-84, doi:10.1097/00007435-198304000-00007 (1983).

287 23 Mortimer, T. D. *et al.* The Distribution and Spread of Susceptible and Resistant
288 *Neisseria gonorrhoeae* Across Demographic Groups in a Major Metropolitan
289 Center. *Clinical infectious diseases : an official publication of the Infectious
290 Diseases Society of America* **73**, e3146-e3155, doi:10.1093/cid/ciaa1229 (2021).

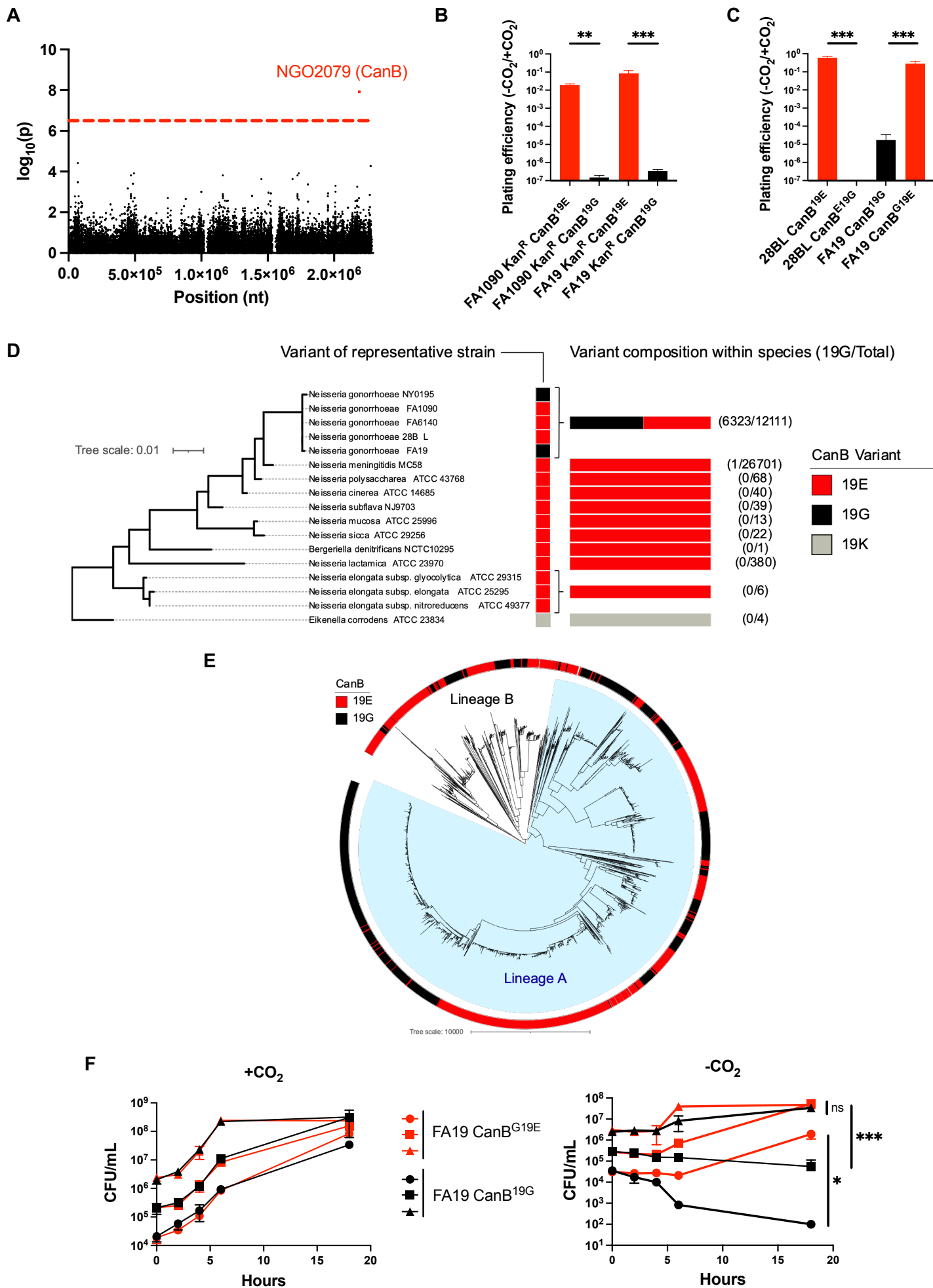
291 24 Zampieri, M. *et al.* Metabolic constraints on the evolution of antibiotic resistance.
292 *Mol Syst Biol* **13**, 917, doi:10.15252/msb.20167028 (2017).

293 25 Pinheiro, F., Warsi, O., Andersson, D. I. & Lässig, M. Metabolic fitness landscapes
294 predict the evolution of antibiotic resistance. *Nat Ecol Evol* **5**, 677-687,
295 doi:10.1038/s41559-021-01397-0 (2021).

296 26 Fung-Tomc, J., Kolek, B. & Bonner, D. P. Ciprofloxacin-induced, low-level
297 resistance to structurally unrelated antibiotics in *Pseudomonas aeruginosa* and
298 methicillin-resistant *Staphylococcus aureus*. *Antimicrobial agents and
299 chemotherapy* **37**, 1289-1296, doi:10.1128/aac.37.6.1289 (1993).

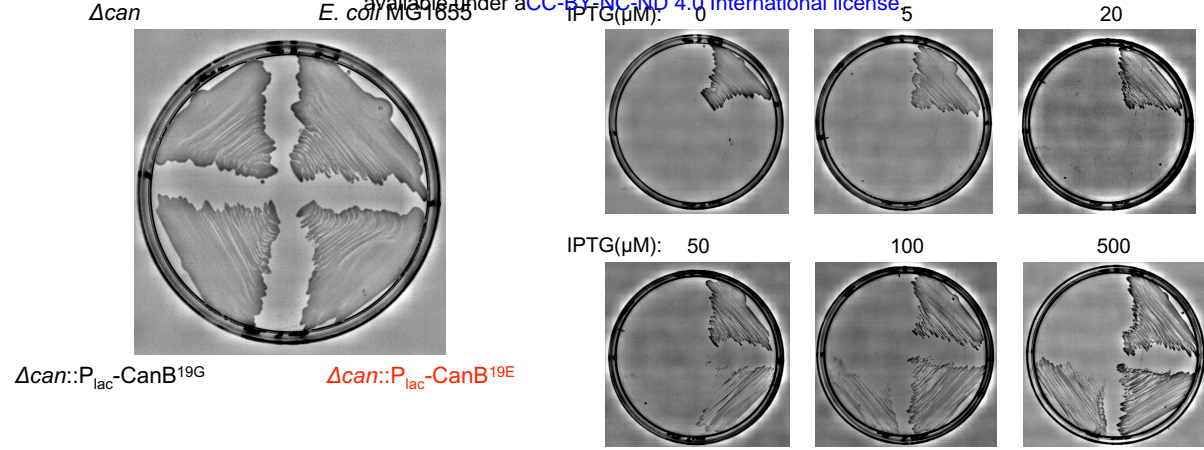
300 27 Yao, J., Bruhn, D. F., Frank, M. W., Lee, R. E. & Rock, C. O. Activation of
301 Exogenous Fatty Acids to Acyl-Acyl Carrier Protein Cannot Bypass FabI Inhibition
302 in *Neisseria*. *The Journal of Biological Chemistry* **291**, 171-181,
303 doi:10.1074/jbc.M115.699462 (2016).

304

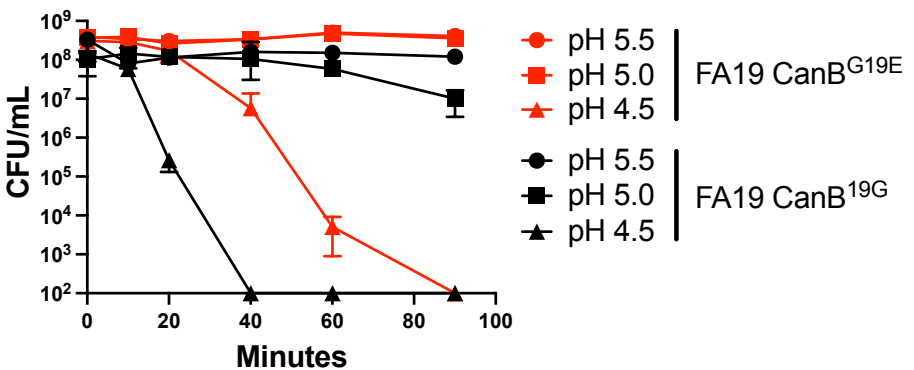


1 **Figure 1.** A SNP in *ngo2079*, encoding a β -carbonic anhydrase, is necessary and sufficient to
2 explain dependence on supplemental CO₂ in *N. gonorrhoeae*. **(A)** Manhattan plot of SNPs
3 associated with dependence on supplemental CO₂ across 30 strains of *N. gonorrhoeae*. Dotted
4 line represents a p-value of 0.05 with Bonferroni correction for 57,691 unitigs. **(B)** Plating
5 efficiencies in the absence and presence of 5% supplemental CO₂ of CanB variants introduced
6 by kanamycin co-selection in *N. gonorrhoeae* strains FA1090 (parental CanB^{19E}) and FA19
7 (parental CanB^{19G}) (N ≥ 6 from two independent experiments). Significance determined by
8 Mann-Whitney U test. **(C)** Plating efficiencies as in **(B)** of *N. gonorrhoeae* strains 28BL (parental
9 CanB^{19E}) and FA19 (parental CanB^{19G}) with isogenic CanB mutants (N ≥ 6 from two
10 independent experiments). Significance determined by Mann-Whitney U test. **(D)**
11 NGO2079/CanB variants across sequenced *Neisseria* and related species represented
12 alongside a 16S maximum-likelihood tree. Branch length represents number of substitutions per
13 site. **(E)** Maximum-likelihood phylogenetic tree of 5,007 strains of *N. gonorrhoeae* with a colored
14 track representing CanB variant. Branch length represents total number of substitutions after
15 removal of predicted recombinations. Lineage A represents isolates that arose
16 phylogeographically After the introduction of *N. gonorrhoeae* into Asia, while Lineage B
17 represents isolates that arose Before that breakpoint, as defined by Sánchez-Busó *et al.*⁵ **(F)**
18 Growth of FA19 CanB isogenic strains in the presence and absence of supplemental CO₂ (N=3,
19 representative of two independent experiments). Significance at 18 hours determined by
20 unpaired two-sided t-test. *p<0.05, **p<0.01, ***p<0.001

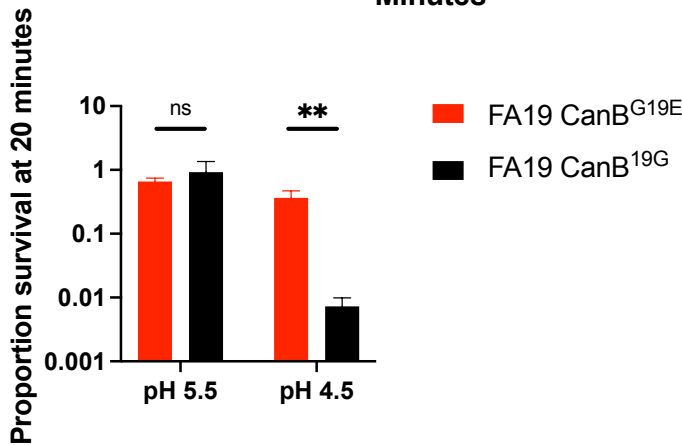
A



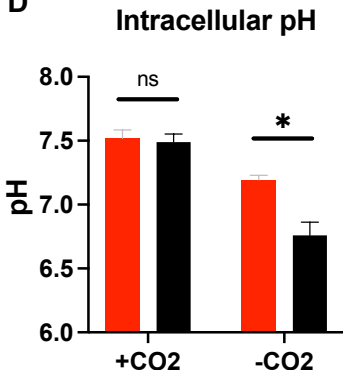
B



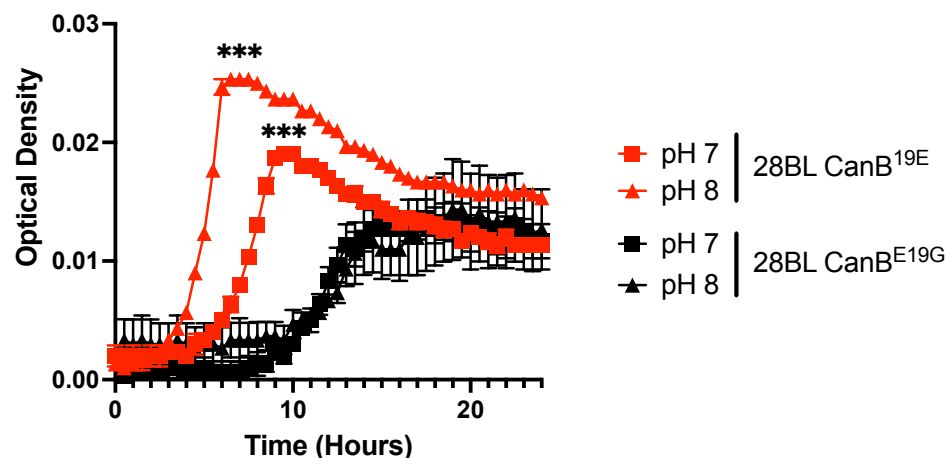
C



D



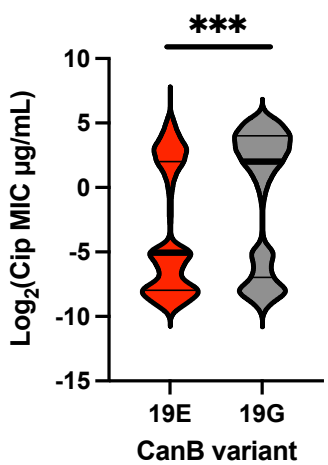
E



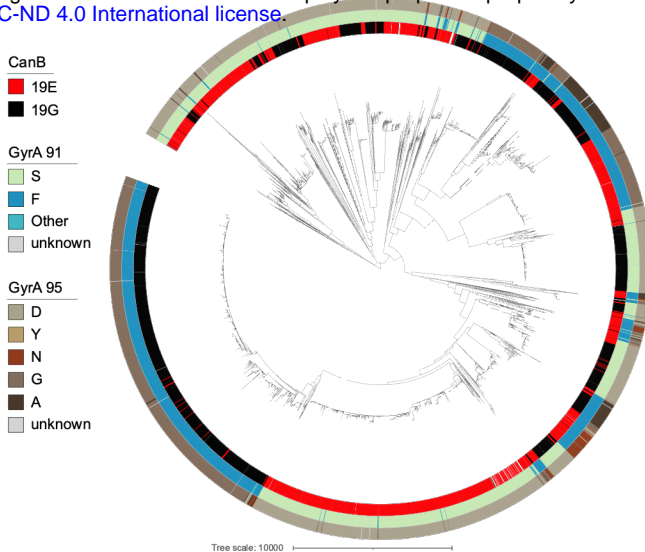
21 **Figure 2.** The 19G variant of CanB is a functional hypomorph. **(A)** Growth of parental *E. coli*
22 MG1655, MG1655 Δ can, and MG1655 Δ can complemented with CanB variants under different
23 levels of induction. **(B)** Survival curve under multiple low pH conditions of FA19 isogenic CanB
24 isolates in monoculture (N=3, representative of three independent experiments). **(C)** As in **(B)**,
25 survival at 20 minutes of exposure to low pH conditions (N=6, from two independent
26 experiments). Significance by Mann-Whitney U test. **(D)** Intracellular pH of FA19 CanB^{19G} and
27 FA19 CanB^{G19E} as measured by flourimetric dye in the presence and absence of supplemental
28 CO₂ (N=3, representative of two independent experiments). **(E)** Growth of the 28BL CanB
29 isogenic pair in liquid culture under anaerobic conditions (N=3, representative of two
30 independent experiments). Significance by unpaired two-sided t-test. *p<0.05, **p<0.01,
31 ***p<0.001

32

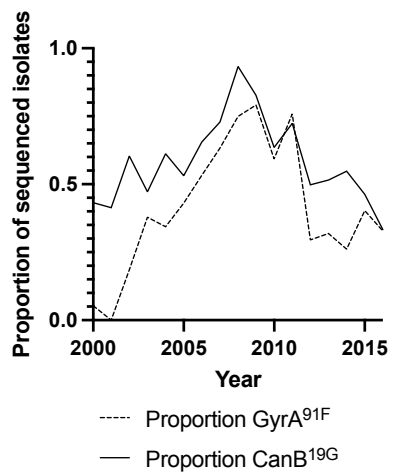
A



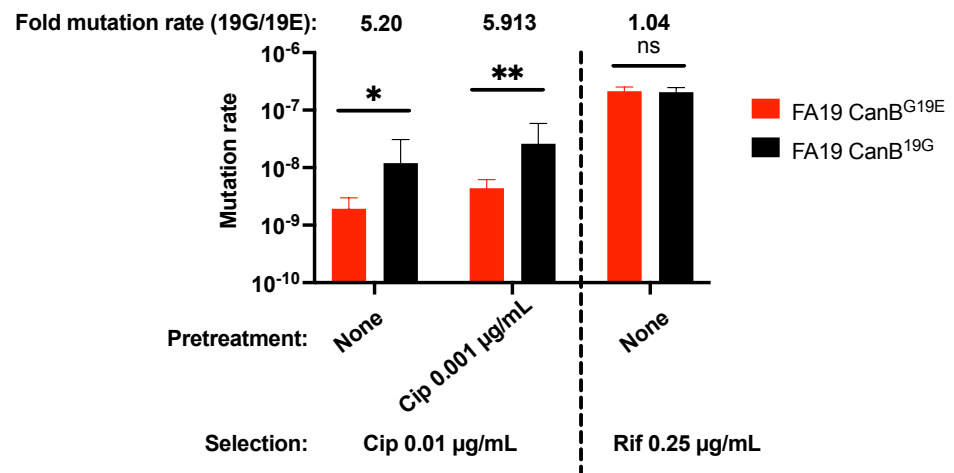
B



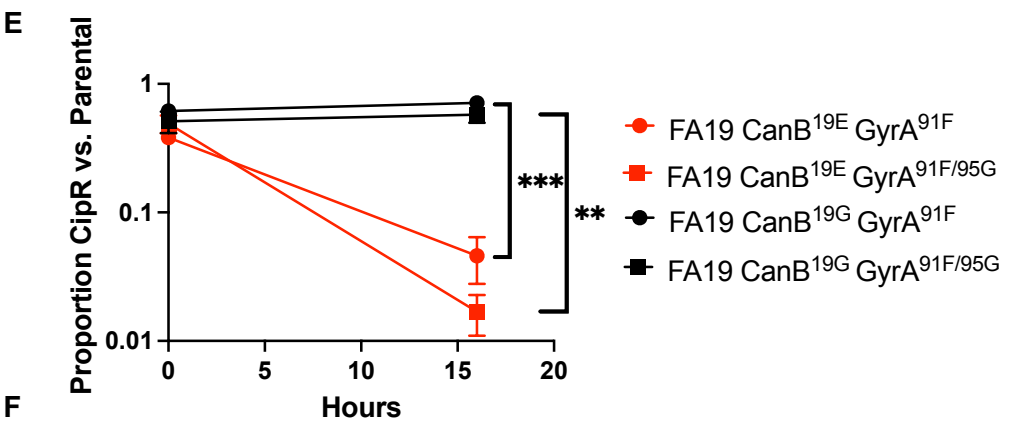
C



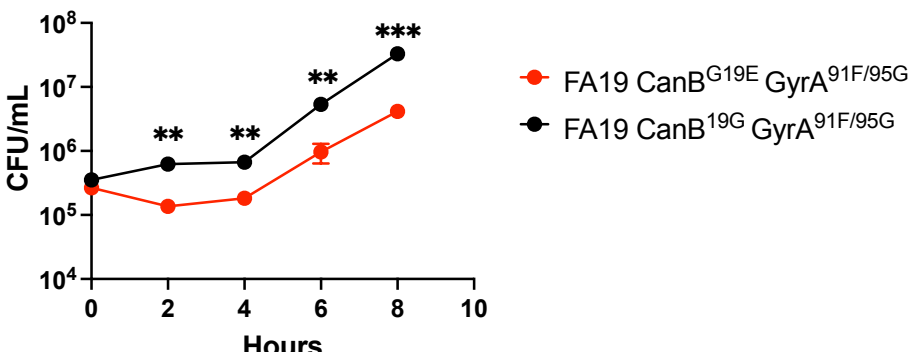
D



E



F



33 **Figure 3.** The CanB^{19G} variant facilitates acquisition of ciprofloxacin resistance. **(A)** Violin plot
34 of ciprofloxacin MICs for 8,912 *N. gonorrhoeae* clinical isolates. Thick lines represent median,
35 thin lines represent 25th/75th percentiles. Significance by Mann-Whitney U test. **(B)** Maximum-
36 likelihood tree, as in **Figure 1C**, overlaid with tracks representing ciprofloxacin conferring
37 variants of GyrA. **(C)** Proportion of sequenced U.S. isolates stratified by year that have the
38 CanB^{19G} variant and the ciprofloxacin resistance-conferring GyrA^{91F} variant. **(D)** Calculated
39 mutation rates to ciprofloxacin and rifampin by fluctuation analysis of isogenic CanB strains +/-
40 pretreatment with sub-MIC ciprofloxacin. Significance by unpaired two sample t-test (N=144,
41 representative of two independent experiments). **(E)** Competition between ciprofloxacin
42 resistant isogenic CanB strains and susceptible parental strains (N=3, representative of two
43 independent experiments). Significance by unpaired two sample t-test. **(F)** Growth curves of
44 CanB isogenic FA19 strains with ciprofloxacin resistance-determining *gyrA* alleles (N=3,
45 representative of two independent experiments). Significance by unpaired two sample t-test.
46 *p<0.05, **p<0.01, ***p<0.001